Supporting Information

Cross-linked $K_{0.5}MnO_2$ Nanoflower Composites for High Rate and Low Overpotential Li–CO_2 Batteries

Jiawei Wu,[a,c ‡] Jian Chen,[b‡] Xiaoyang Chen,[b] Yang Liu,[a,b *] Zhe Hu,[d] Feijian Lou,[a*] Shulei Chou[e] and Yun Qiao[a,b*]

[a] School of Chemistry and Chemical Engineering, Henan Normal University, Xinxiang, Henan 453007, China. E-mail address: liuy986@htu.edu.cn; loufeijian@htu.edu.cn;

[b] School of Environment and Chemical Engineering, Shanghai University, Shanghai 200444, China. E-mail address: yunqiao@shu.edu.cn

[c] Sinopec Petroleum Engineering Zhongyuan Co. Ltd., Natural Gas Technology Center, Zhengzhou, Henan 450000, China

[d] College of Materials Science and Engineering, Shenzhen University, Shenzhen 518055, China

[e] Institute for Carbon Neutralization, College of Chemistry and Materials Engineering, Wenzhou University, Wenzhou, Zhejiang 325035, China.

[‡] J. Wu and. J. Chen. contributed equally to this work.

Experimental

Materials

Potassium permanganate ($KMnO_4$), lithium bis(trifluoromethane sulfonimide) (LiTFSI), tetraethylene glycol dimethyl ether (TEGDME) and N-methyl-2-pyrrolidone (NMP) were purchased from Aladdin Ltd. Sulfuric acid (H_2SO_4, 98%), nitric acid (HNO_3, 60%) were purchased from Guoyao Chemical Reagent Co., Ltd. multi-wall carbon nanotubes (CNT) were brought from XFNANO Co., Ltd.

Preparation of $K_{0.5}MnO_2$/CNT.

First, CNT were functionalized via acid treatment to enhance their hydrophilicity. The CNT were treated at 80 °C for 8 h in a mixed acid solution of H_2SO_4 and HNO_3 with the volume ratio of 3:1. Thereafter, 20 mg of the functionalized CNT were dispersed into 8 mmol L^{-1} potassium permanganate solution, ultrasonicated and stirred for 1 h. And then, the mixed solution was transferred into a 100 mL polytetrafluoroethylene stainless steel autoclave and kept at 140 °C for 2 h. At last, the product was washed several times with deionized water and ethanol and dried under vacuum at 60 °C, the as-obtained sample was labeled as $K_{0.5}MnO_2$/CNT composite.

Materials Characterization.

The morphology and the energy-dispersive X-ray spectroscopy (EDS) spectrum of the samples were characterized by scanning electron microscopy (FE-SEM) (Hitachi SU8010). TEM and high-resolution transmission electron microscopy (HRTEM) were recorded on a JEM-ARM300F. The high-angle-annular dark-field scanning transmission electron microscopy (HAADF-STEM) and the corresponding EDS elemental mapping were performed on FEI Themis Z. X-ray diffraction (XRD) patterns were measured on a X' Pert3 Powder diffractometer with Cu Kα radiation (λ=1.54 Å). Inductively coupled plasma (ICP) analysis was carried out by using Prodigy 7. X-ray photoelectron spectroscopy (XPS) was conducted on an ESCALAB 250Xi X-ray Photoelectron Spectrometer. Raman spectra were token on a Horiba LabRAM HR Evolution using a 532 nm laser.

Battery Assemble and Electrochemical Tests.

First, for the cathode preparation, 90 wt% $K_{0.5}MnO_2$/CNT and 10 wt%

polyvinylidene fluoride (PVDF) were dispersed in the NMP solution. Then, the slurry was uniformly coated on carbon paper and dried under vacuum at 80 °C overnight. The Li–CO_2 batteries were assembled in a glove box filled with pure argon. The $K_{0.5}MnO_2$/CNT cathode and the lithium anode were separated by a glass fiber separator impregnated with 50 μL electrolyte (1.0 M LiTFSI/TEGDME), and sealed into a CR2032-type coin cell. Then, the battery was transferred into a glove box filled with pure CO_2. Finally, the galvanostatic discharge/charge measurements were performed on the LAND-CTA2001A test system. The cyclic voltammetry curves were obtained on the CHI760E electrochemical workstation.

Theoretical calculation.

DFT calculations were conducted using Vienna ab initio Simulation Package (VASP). [1,2] The projector-augmented wave method was used for the electron−ion interactions with a cut-off energy of 520 eV. [3] Generalized gradient approximation with the Perdew−Burke−Ernzerhof function was used to approximate exchange correlation energy. [4] The k-point grid was set as 3 × 3 × 1. Atomic positions and cell vectors were fully optimized until all force components were less than 0.02 eV $Å^{-1}$.

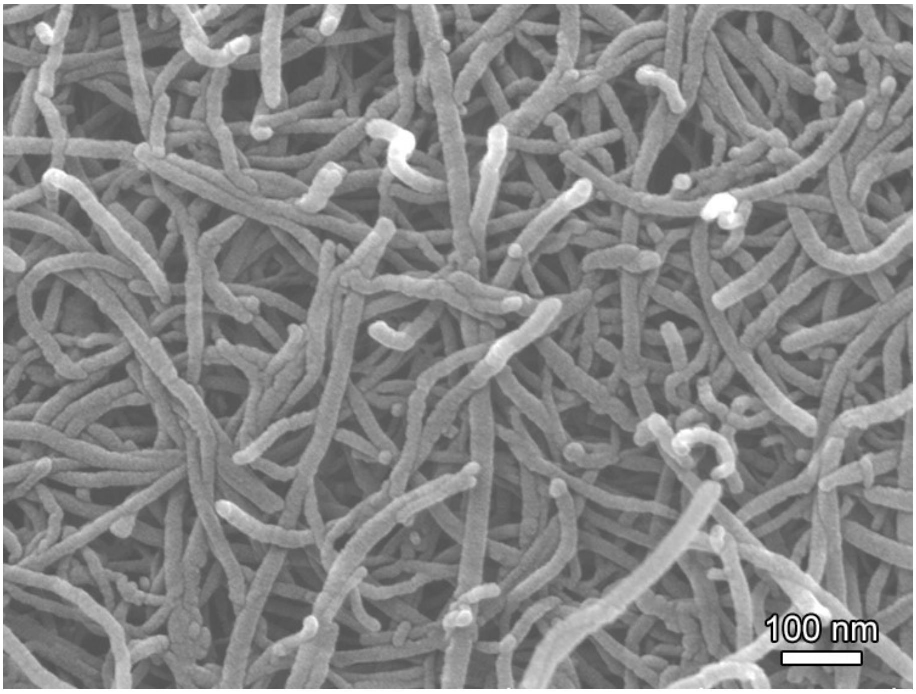

Fig. S1. SEM image of the pristine CNT.

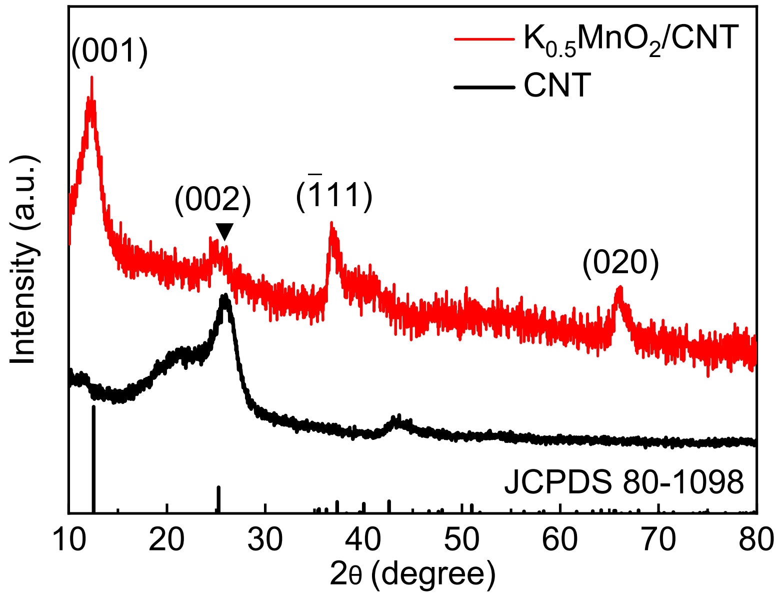

Fig. S2. (a) XRD patterns of the $K_{0.5}MnO_2$/CNT and pure CNT.

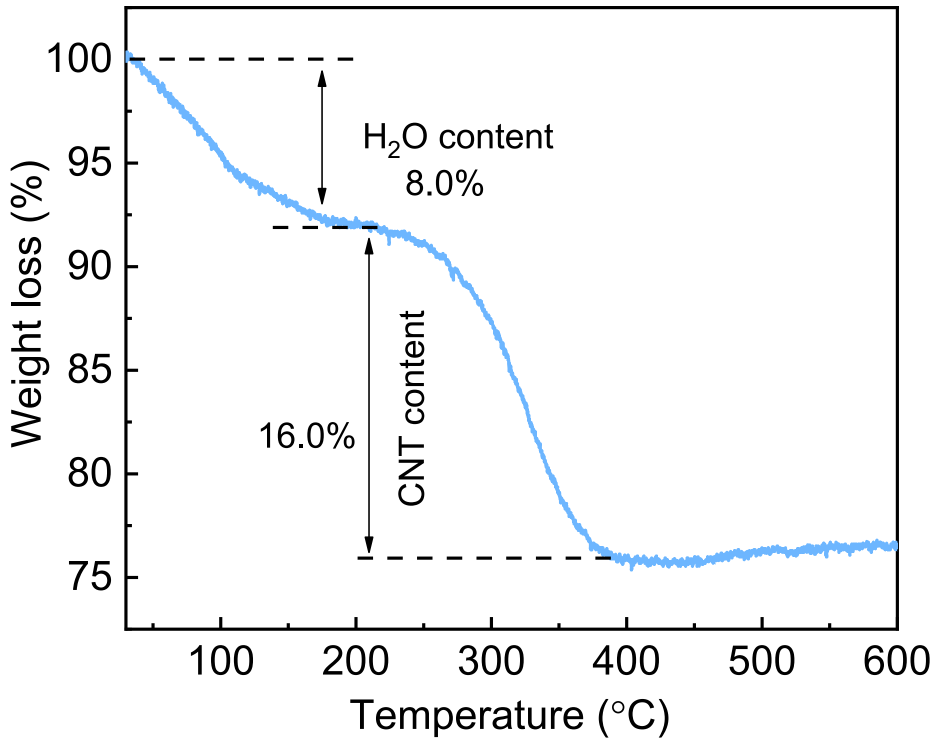

Fig. S3. Thermogravimetric analysis for the proportion of CNT in the $K_{0.5}MnO_2$/CNT composite.

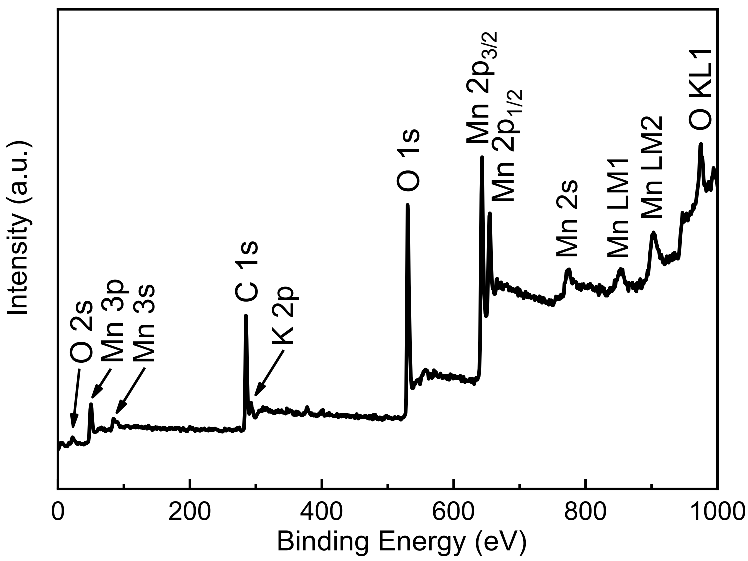

Fig. S4. The XPS survey spectrum of $K_{0.5}MnO_2$/CNT.

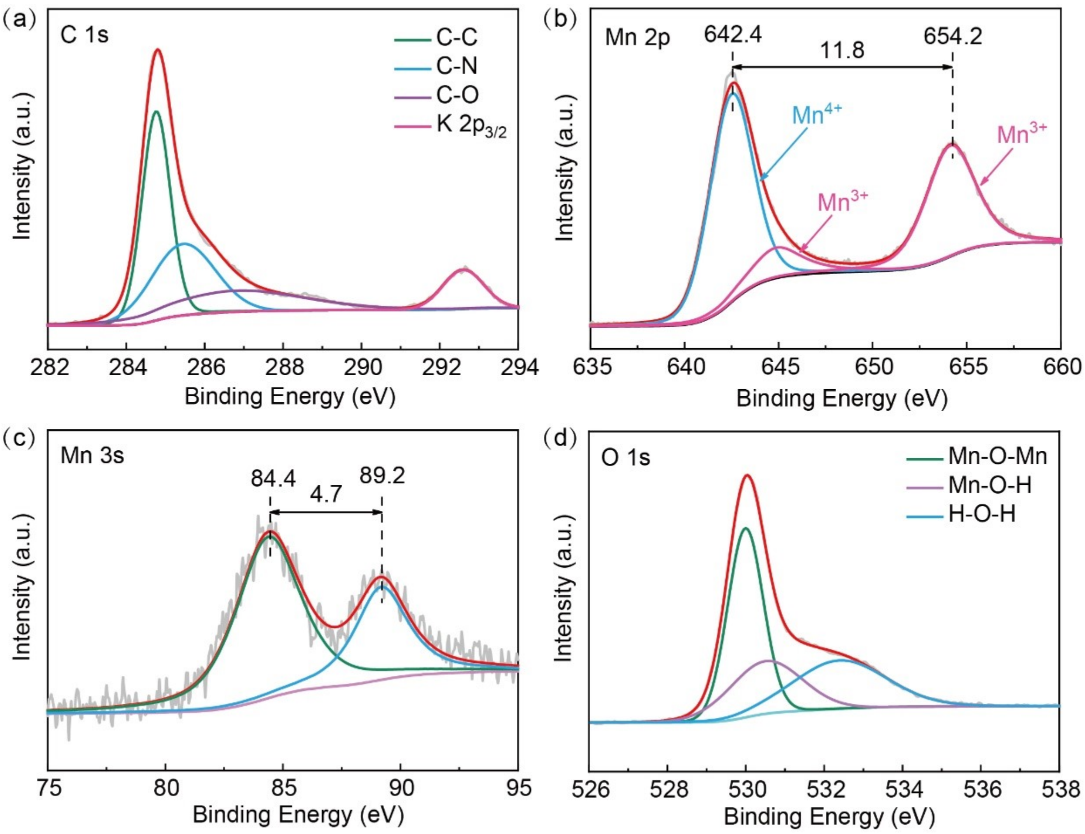

Fig. S5. High-resolution XPS spectra of (a) C 1s, (b) Mn 2p, (c) Mn 3s and (d) O 1s for the $K_{0.5}MnO_2$/CNT sample.

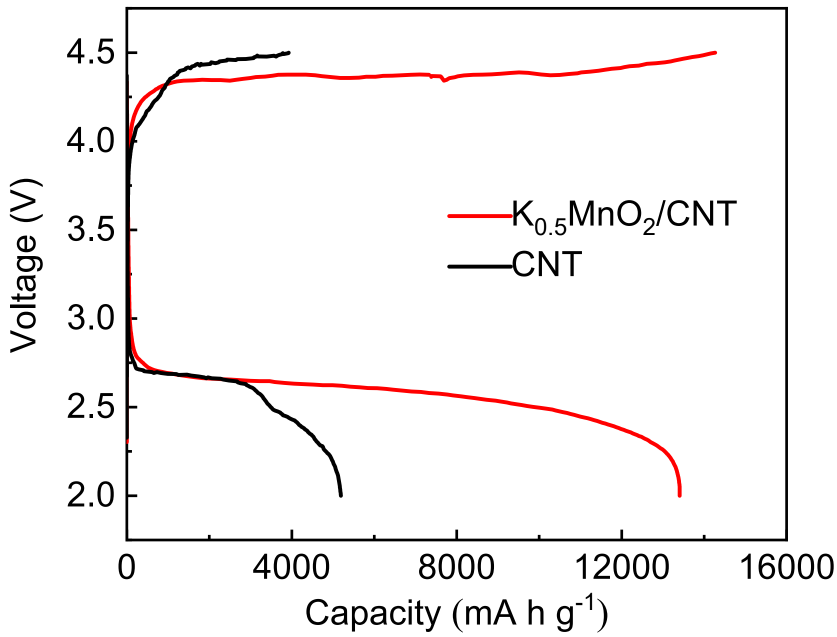

Fig. S6. Discharge/charge curves of Li-CO_2 battery based on $K_{0.5}MnO_2$/CNT and CNT cathodes at 100 mA g^{-1}.

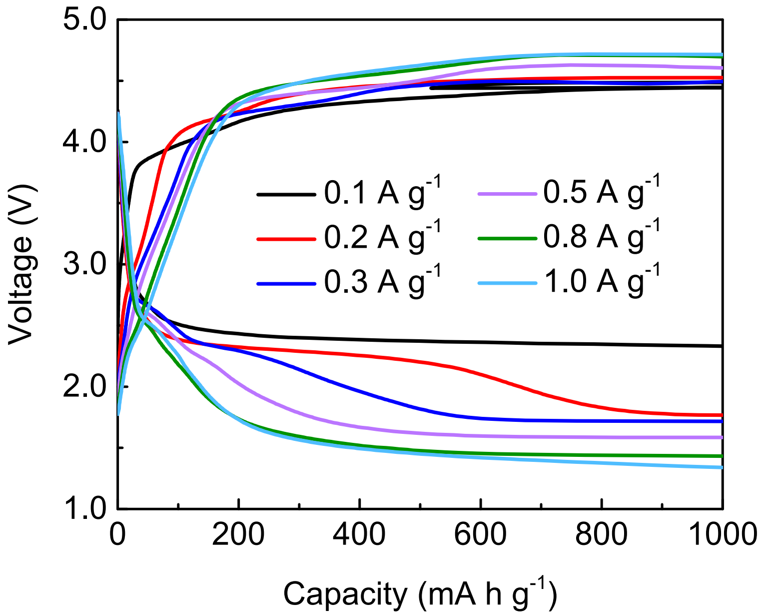

Fig. S7. The charge/discharge profiles of the CNT electrode at various current densities.

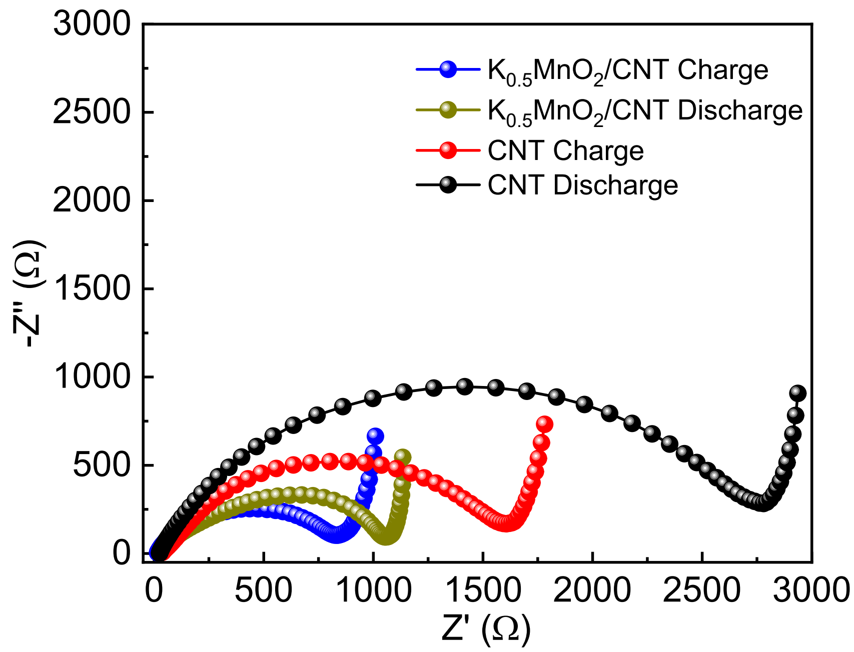

Fig. S8. EIS spectra for $K_{0.5}MnO_2$/CNT and CNT cathodes after the first discharge and charge processes.

Table S1. The element content of K and Mn in the $K_{0.5}MnO_2$/CNT from ICP results.

Elements	K (wt%)	Mn (wt%)
Content	15.15	40.95

Table S2. The electrochemical performance summary and comparison of various Li-CO_2 batteries.

Cathode catalyst	Electrolyte	Discharge/Charge plateau (V)	Cycle capacity/ Current (mA h g^{-1}/ mA g^{-1})	Cycle number (n)	Capacity (mA h g^{-1})	Energy efficiency (%)	Reference
$K_{0.5}MnO_2$/CNT	LiTFSI in TEGDME	2.86/3.91	1000/100	100	14267	87.95	this work
CNT	LiTFSI in TEGDME	2.7/4.3	1000/50	29	8379	63.5	Zhang et al.[5]
Graphene	LiTFSI in TEGDME	2.75/4.2	1000/100	10	14722	N/A	Zhang et al.[6]
BN-hG	LiTFSI in TEGDME	2.92/4.0	1000/100	200	16033	N/A	Qie et al.[7]
Ni/NG	LiTFSI in TEGDME	2.5<V<4.2	1000/100	101	17625	67.5	Zhang et al.[8]
Cu/NG	LiTFSI in TEGDME	2.85/3.62	1000/200	50	13590	N/A	Zhang et al.[9]
Ni/r-GO	LiTFSI in TEGDME	2.7/4.0	1000/100	100	14.6 mA h cm^{-2}	N/A	Qiao et al.[10]
Ir/CNFs	LiTFSI in TEGDME	2.76/4.14	1000/50	45	21528	N/A	Wang et al.[11]
Ir/N-CNFs	LiTFSI in TEGDME	2.75/3.8	1000/500	400	7667	N/A	Xing et al.[12]
NiO/CNT	LiTFSI in TEGDME	2.7/4.1	1000/50	42	9000	66	Zhang et al.[13]
P-Mn_2O_3/KB	$LiClO_4$ in	2.5/4.3	1000/50	45	9434	N/A	Ma et al.[14]

	TEGDME						
Mn-MOF	LiTFSI in TEGDME	2.6/4.46	1000/200	50	18022	N/A	Li et al.[15]
Mo_2C/CNT	$LiCF_3SO_3$ in TEGDME	2.5/3.45	100μAh cm^{-2}/20μA	40	287.5	77	Hou et al.[16]
CQD/hg	LiTFSI in DMSO with 0.3M $LiNO_3$	3.0/4.0	500/1000	235	12300	74.3	Jin et al.[17]
Ru/Ni foam	LiTFSI in TEGDME	2.8/4.0	1000/200	100	9502	N/A	Zhao et al.[18]
Ru/N-doped CNT	LiTFSI in TEGDME	2.35/4.1	500/100	150	9300	N/A	Zhang et al.[19]
Ru/ACNF	LiTFSI in TEGDME	2.8/4.15	1000/100	50	11495	N/A	Qiao et al.[20]
RuP_2/NPCF	LiTFSI in TEGDME	2.7/4.0	1000/200	200	11951	N/A	Guo et al.[21]
CNT@RuO_2	LiTFSI in TEGDME	2.46/3.97	500/50 500/100 500/150	55 30 20	2187	N/A	Bie et al.[22]
RuO_2/LDO/Ni foam	LiTFSI in TEGDME	2.52/3.25	1000/166	60	5455	N/A	Xu et al.[23]
ZnS QDs/N-rGO	LiTFSI in TEGDME	2.75/4.13	1000/400	190	10310	N/A	Wang et al.[24]
N-CNTs@Ti	LiTFSI in TEGDME	2.73/4.24	1000/250	45	9292.3	65	Li et al.[25]
Pt-based LCB	LiTFSI in TEGDME	2.56/2.91	1000/100	100	41470	89.5	Wang et al.[26]
Porous Pt @	LiTFSI in	2.55/3.0	100μAh	>200	5.81 mAh	87.6	Chen et al.[27]

carbon cloth	TEGDME		cm^{-2}/20μA		cm^{-2}		
IrRu/N-CNT	LiTFSI in TEGDME	2.6/ 3.8	500/100	600	6628	68.4*	Wang et al.[28]
Cd SAs/NC	LiTFSI in DMSO+0.3 M $LiNO_3$	2.91/4.22	500/1000	1685	160045	70.4*	Zhu et al.[29]
$SnCu_{1.5}O_{3.5}$@MFI	LiTFSI in TEGDME	2.34/4.02	1000/100	100	23000	58.2*	Zhu et al.[30]
TiVC/rGO aerogels	$LiCF_3SO_3$ in TEGDME	2.77/4.18	1000/20	91	27880	66.3*	Zhao et al.[31]
MOC@NCNF	N/A	2.58/4.03	100μAh cm^{-2}/20μA	171	10.31 mAh cm^{-2}	64.94	Liu et al.[32]
S_V-CoS	LiTFSI in TEGDME	3.07/3.5*	100μAh cm^{-2}/20μA	40	7790.6 μAh cm^{-2}	89.1	Mao et al.[33]

Note: * denotes the energy efficiency value calculated from performance data reported in the literature.

REFERENCES

[1] Kresse, G.; Hafner, J. Phys. Rev. B **1994**, 49, 14251–14269.

[2] Kresse, G.; Furthmüller, J. Comput. Mater. Sci. **1996**, 6, 15–50.

[3] Blöchl, P. E. Phys. Rev. B **1994**, 50, 17953–17979.

[4] Perdew, J. P.; Yue, W. Phys. Rev. B **1986**, 33, 8800–8802.

[5] Zhang, X.; Zhang, Q.; Zhang, Z.; Chen, Y.; Xie, Z.; Wei, J.; Zhou, Z., Chem. Commun. **2015,** *51*, 14636-14639.

[6] Zhang, Z.; Zhang, Q.; Chen, Y.; Bao, J.; Zhou, X.; Xie, Z.; Wei, J.; Zhou, Z., *Angew. Chem. Int. Ed.* **2015,** *54*, 6550-6553.

[7] Qie, L.; Lin, Y.; Connell, J. W.; Xu, J.; Dai, L., *Angew. Chem. Int. Ed.* **2017,** *56*, 6970-6974.

[8] Zhang, Z.; Wang, X. G.; Zhang, X.; Xie, Z.; Chen, Y. N.; Ma, L.; Peng, Z.; Zhou, Z., Adv. Sci. **2018,** *5*, 1700567.

[9] Zhang, Z.; Zhang, Z. W.; Liu, P. F.; Xie, Y. P.; Cao, K. Z.; Zhou, Z., J. Mater. Chem. A **2018,** *6*, 3218-3223.

[10] Qiao, Y.; Liu, Y.; Chen, C.; Xie, H.; Yao, Y.; He, S.; Ping, W.; Liu, B.; Hu, L., Adv. Funct. Mater. **2018,** *28*, 1805899.

[11] Wang, C.; Zhang, Q.; Zhang, X.; Wang, X. G.; Xie, Z.; Zhou, Z., Small **2018,** *14*, 1800641.

[12] Xing, Y.; Yang, Y.; Li, D.; Luo, M.; Chen, N.; Ye, Y.; Qian, J.; Li, L.; Yang, D.; Wu, F.; Chen, R.; Guo, S., Adv. Mater. **2018,** *30*, 1803124.

[13] Zhang, X.; Wang, C. Y.; Li, H. H.; Wang, X. G.; Chen, Y. N.; Xie, Z. J.; Zhou, Z., J. Mater. Chem. A **2018,** *6*, 2792-2796.

[14] Ma, W.; Lu, S.; Lei, X.; Liu, X.; Ding, Y., Porous Mn_2O_3 cathode for highly durable Li–CO_2 batteries. J. Mater. Chem. A **2018,** *6*, 20829-20835.

[15] Li, S. W.; Dong, Y.; Zhou, J. W.; Liu, Y.; Wang, J. M.; Gao, X.; Han, Y. Z.; Qi, P. F.; Wang, B., Energy Environ. Sci **2018,** *11*, 1318-1325.

[16] Hou, Y.; Wang, J.; Liu, L.; Liu, Y.; Chou, S.; Shi, D.; Liu, H.; Wu, Y.; Zhang, W.; Chen, J., Adv. Funct. Mater. **2017,** *27*, 1700564.

[17] Jin, Y.; Hu, C.; Dai, Q.; Xiao, Y.; Lin, Y.; Connell, J. W.; Chen, F.; Dai, L., Adv.

Funct. Mater. **2018,** *28*, 1804630.
[18] Zhao, H. M.; Li, D. D.; Li, H. D.; Tamirat, A. G.; Song, X. Y.; Zhang, Z. X.; Wang, Y. G.; Guo, Z. Y.; Wang, L.; Feng, S. H., Electrochim. Acta **2019,** *299*, 592-599.
[19] Zhang, P.-F.; Lu, Y.-Q.; Wu, Y.-J.; Yin, Z.-W.; Li, J.-T.; Zhou, Y.; Hong, Y.-H.; Li, Y.-Y.; Huang, L.; Sun, S.-G., Chem. Eng. J **2019,** *363*, 224-233.
[20] Qiao, Y.; Xu, S.; Liu, Y.; Dai, J.; Xie, H.; Yao, Y.; Mu, X.; Chen, C.; Kline, D. J.; Hitz, E. M.; Liu, B.; Song, J.; He, P.; Zachariah, M. R.; Hu, L., Energy Environ. Sci. **2019,** *12*, 1100-1107.
[21] Guo, Z.; Li, J.; Qi, H.; Sun, X.; Li, H.; Tamirat, A. G.; Liu, J.; Wang, Y.; Wang, L., Small **2019,** *15*, 1803246.
[22] Bie, S.; Du, M.; He, W.; Zhang, H.; Yu, Z.; Liu, J.; Liu, M.; Yan, W.; Zhou, L.; Zou, Z., ACS Appl. Mater. Interfaces **2019,** *11*, 5146-5151.
[23] Xu, S.-M.; Ren, Z.-C.; Liu, X.; Liang, X.; Wang, K.-X.; Chen, J.-S., Energy Storage Mater. **2018,** *15*, 291-298.
[24] Wang, H.; Xie, K.; You, Y.; Hou, Q.; Zhang, K.; Li, N.; Yu, W.; Loh, K. P.; Shen, C.; Wei, B., Adv. Energy Mater. **2019,** *9*, 1901806.
[25] Li, Y.; Zhou, J.; Zhang, T.; Wang, T.; Li, X.; Jia, Y.; Cheng, J.; Guan, Q.; Liu, E.; Peng, H.; Wang, B., Adv. Funct. Mater. **2019,** *29*, 1808117.
[26] Wang, M.; Yang, K.; Ji, Y.; Liao, X.; Zhang, G.; Masteghin, M. G.; Peng, N.; Richheimer, F.; Li, H.; Wang, J.; Liu, X.; Yang, S.; Petrucco, E.; Shearing, P.; Castro, F. A.; Silva, S. R. P.; Zhao, Y.; Pan, F.; Zhao, Y. Energy Environ. Sci. **2023**, *16*, 3960–3967.
[27] Chen, S.; Yang, K.; Zhu, H.; Wang, J.; Gong, Y.; Li, H.; Wang, M.; Zhao, W.; Ji, Y.; Pan, F.; Silva, S. R. P.; Zhao, Y.; Yang, L. Nano Energy **2023**, *117*, 108872.
[28] Wang, Z.; Liu, B.; Yang, X.; Zhao, C.; Dong, P.; Li, X.; Zhang, Y.; Doyle-Davis, K.; Zeng, X.; Zhang, Y.; Sun, X. Adv. Funct. Mater. **2023**, *33*, 2213931.
[29] Zhu, K.; Li, X.; Choi, J.; Choi, C.; Hong, S.; Tan, X.; Wu, T.-S.; Soo, Y.-L.; Hao, L.; Robertson, A. W.; Jung, Y.; Sun, Z. Adv. Funct. Mater. **2023**, *33*, 2213841.
[30] Zhu, Y.; Li, P.; Yang, X.; Wang, M.; Zhang, Y.; Gao, P.; Huang, Q.; Wei, Y.;

Yang, X.; Wang, D.; Shen, Y.; Wang, M. Adv. Energy Mater. **2023**, *13*, 2204143.
[31] Zhao, W.; Yang, Y.; Deng, Q.; Dai, Q.; Fang, Z.; Fu, X.; Yan, W.; Wu, L.; Zhou, Y. Adv. Funct. Mater. **2023**, *33*, 2210037.
[32] Liu, L.; Shen, S.; Zhao, N.; Zhao, H.; Wang, K.; Cui, X.; Wen, B.; Wang, J.; Xiao, C.; Hu, X.; Su, Y.; Ding, S. Adv. Mater. **2024**, 2403229. DOI: 10.1002/adma.202403229.
[33] Mao, R.; Liu, Y.; Shu, P.; Lu, B.; Chen, B.; Chen, Y.; Song, Y.; Jia, Y.; Zheng, Z.; Peng, Q.; Zhou, G. EcoMat **2024** , e12449. DOI: 10.1002/eom2.12449.